



科学技術と文化総合講義 (宇宙と地球の科学)

片岡龍峰

第10回: 2012年7月16日

「過去最悪の宇宙環境を探る」

授業内容

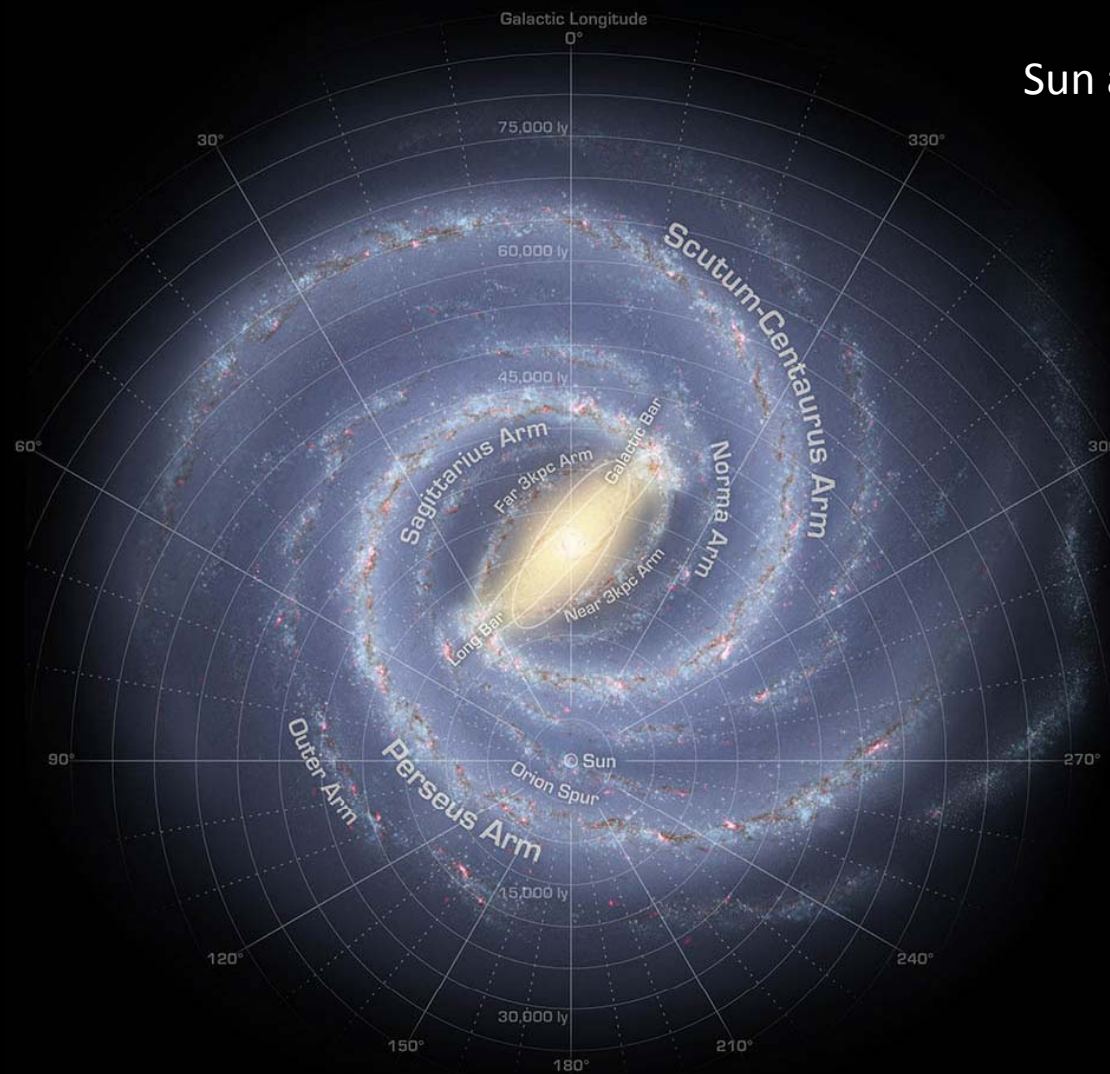
- 1. 授業ガイダンス(オーロラ上映あり) 4月16日
- 2. 太陽地球環境1(大地から太陽系の果てまで)
- 3. 太陽地球環境2(生命を守る3つの盾「太陽風・地磁気・大気」) 4月23日
- 4. 太陽地球環境3(生命を脅かす3つの槍「宇宙線、宇宙塵、太陽紫外線」) 4月30日
- 5. 宇宙災害1(磁気嵐と大停電) 5月7日
- 6. 宇宙災害2(放射線帯と人工衛星障害) 5月21日(休講) 5月14日
- 7. 宇宙災害3(銀河宇宙線と太陽放射線被ばく) 5月28日
- 8. 宇宙天気予報1(世界の宇宙天気モニター) 6月4日
- 9. 宇宙天気予報2(宇宙天気の数値予報) 6月18日(休講) 6月11日
- 10. 太陽気候関係1(マウンダー極小期と魔女狩り) 6月25日(休講)
- 11. 太陽気候関係2(宇宙線雲仮説) 7月2日
- 12. 宇宙史と地球史1(暗い若い太陽のパラドックス) 7月9日
- 13. 宇宙史と地球史2(超新星と大絶滅) 7月16日
- 14. 宇宙史と地球史3(暗黒星雲と雪玉地球) +補講?
- 15. まとめ

* 授業の内容は進み具合や最新の話題に合わせて適宜調整します。

地球史と宇宙史の関係はどうなっているのか

30 kpc x 30 kpc x 200 pc

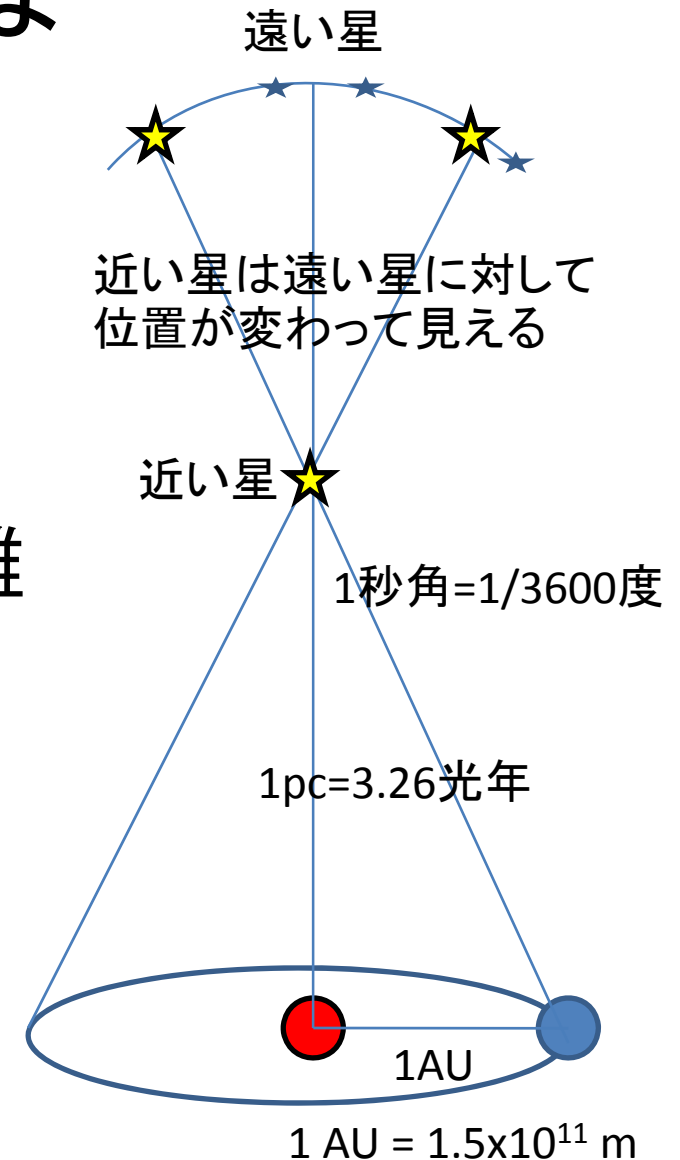
Sun at 8.5 kpc



Annotated Roadmap to the Milky Way
[artist's concept]

パーセクとは

- parsec
 - parallax (視差) + second (秒)
- 年周視差が1秒角になる距離
 - 3.26光年の星でちょうど1秒角
- $1\text{pc} = 3 \times 10^{16} \text{ m} = 0.2 \times 10^6 \text{ AU}$



暗黒星雲と超新星

大量の塵！



暗黒星雲

1-100 pc

10-100 K

100-1000 /cc

20 km/s

1% of mass is dust

Time scale is million years

(a number of geomagnetic excursions occur)

銀河宇宙線の源！



超新星

10-100 pc

10-100 MK

0.01-1 /cc

1000 km/s

10 % of pressure is cosmic rays

Time scale is thousand years

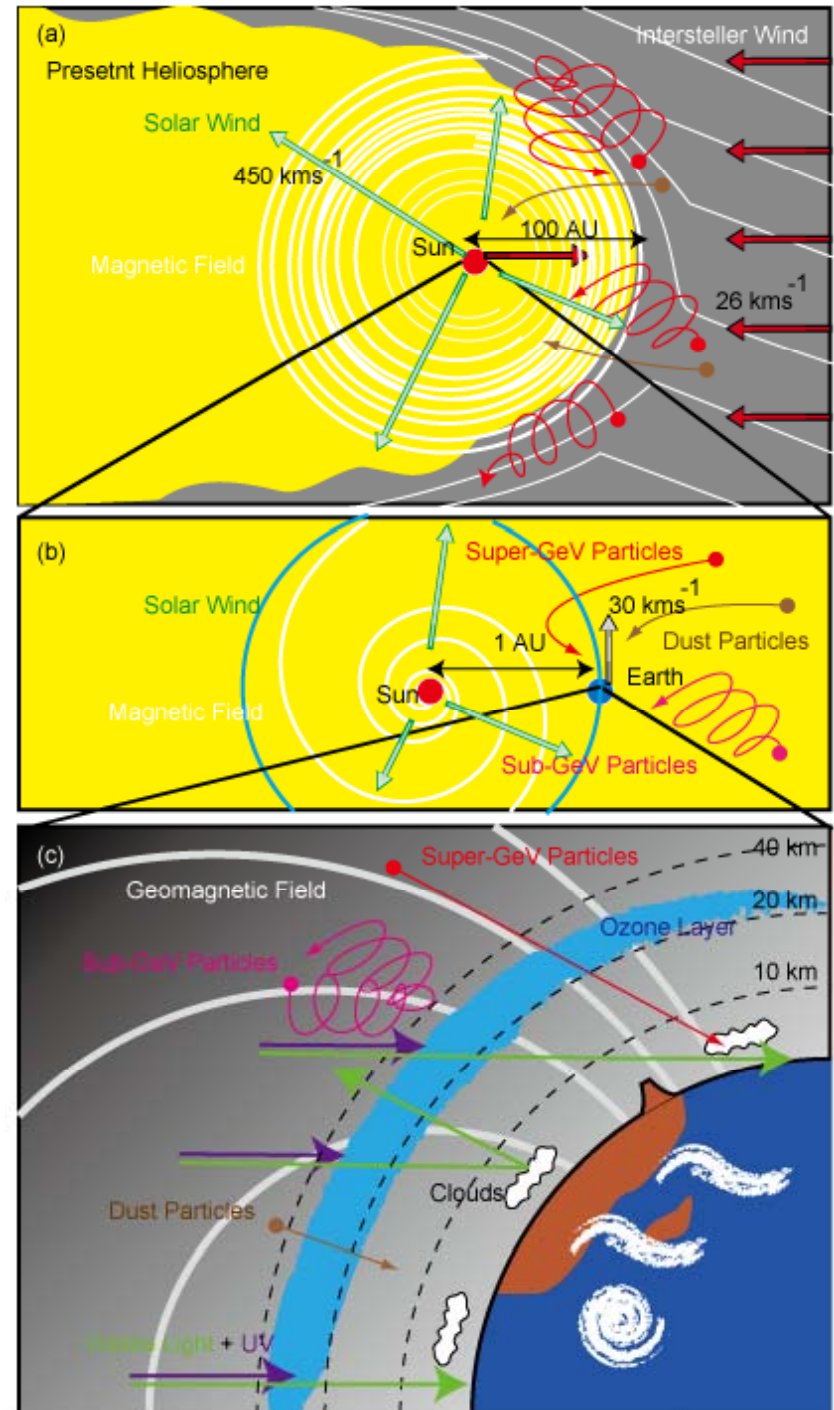
10億年に1回か2回は直撃する(1000/cc DC or 10 pc SNR)

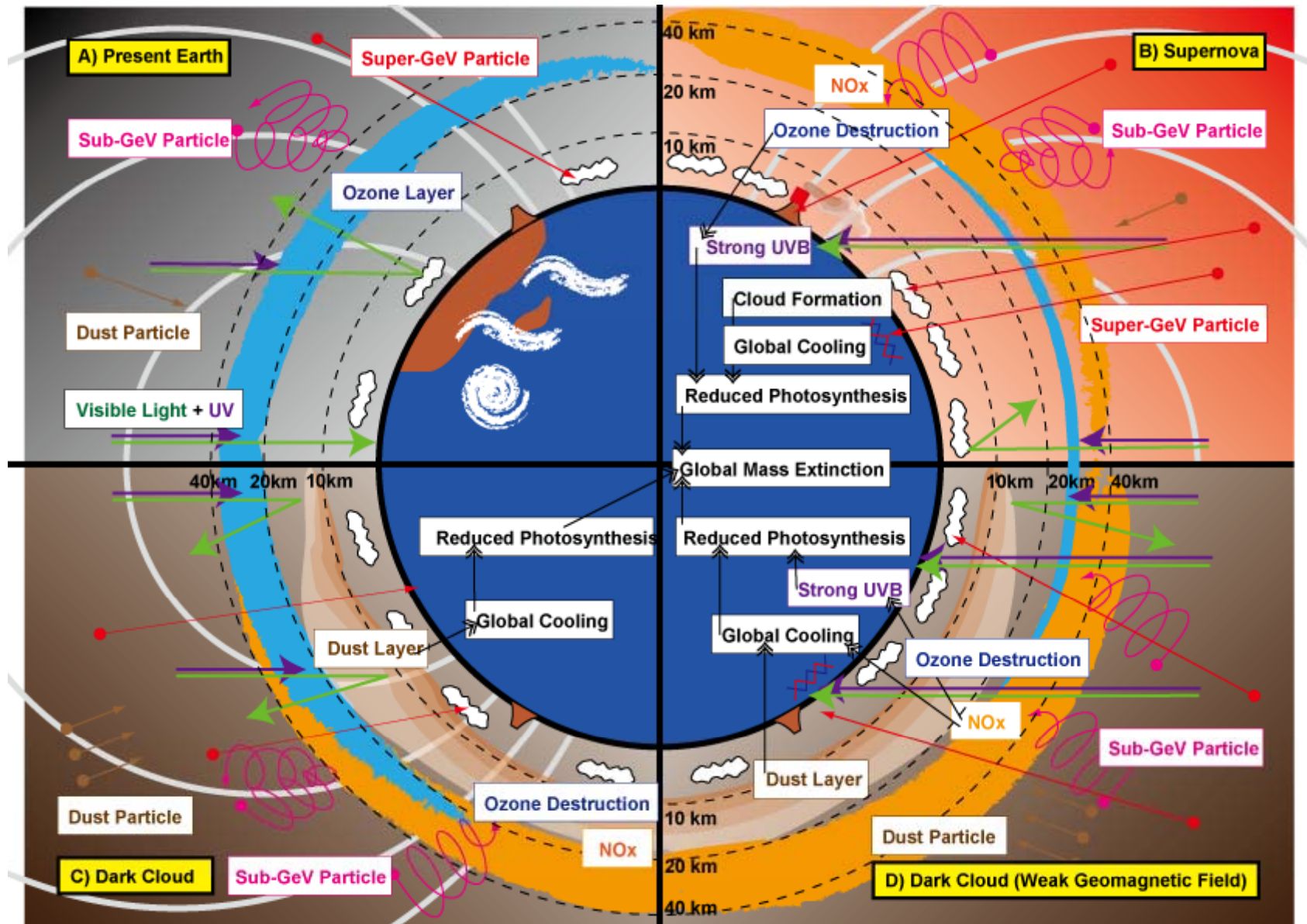
地球が経験した最悪の宇宙環境は？

- 超新星との衝突
 - ガンマ線バーストの放射
- 暗黒星雲との衝突
 - 地磁気反転と同時に発生
- 「3つの槍」と「3つの盾」のバランスが崩れ、地球が凍りつくような気候変動や、大絶滅が起きてきた可能性がある。

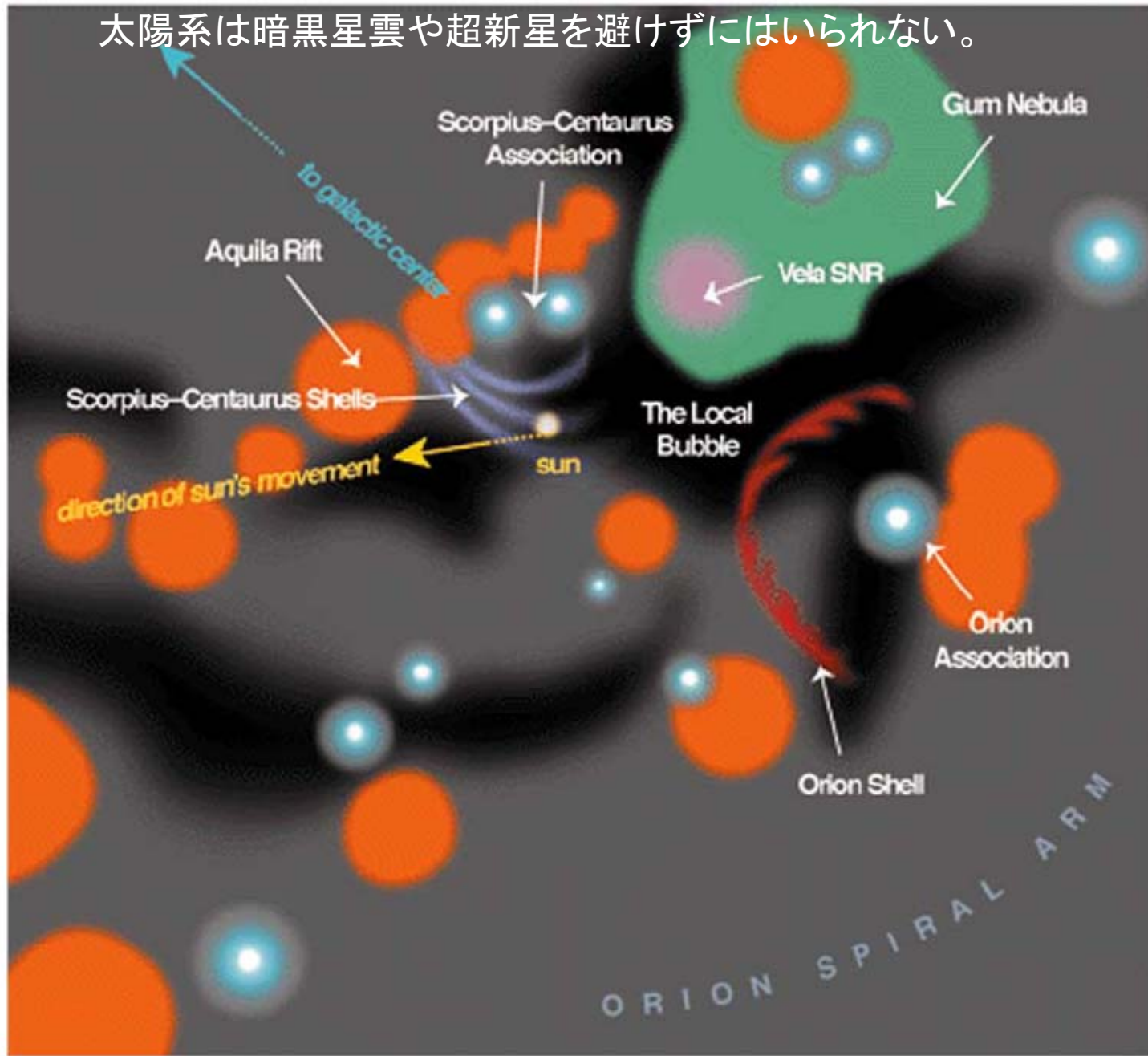
現在の宇宙環境

- 3つの槍がある
 - 宇宙線
 - 宇宙塵
 - 紫外線
- 3つの盾がある
 - 太陽風
 - 地磁気
 - 大気(オゾン層)





太陽系は暗黒星雲や超新星を避けずにはいられない。



■ molecular clouds

■ diffuse gas

400-500 pc view (Frisch 2000)

超新星を起こしてきた近くの星

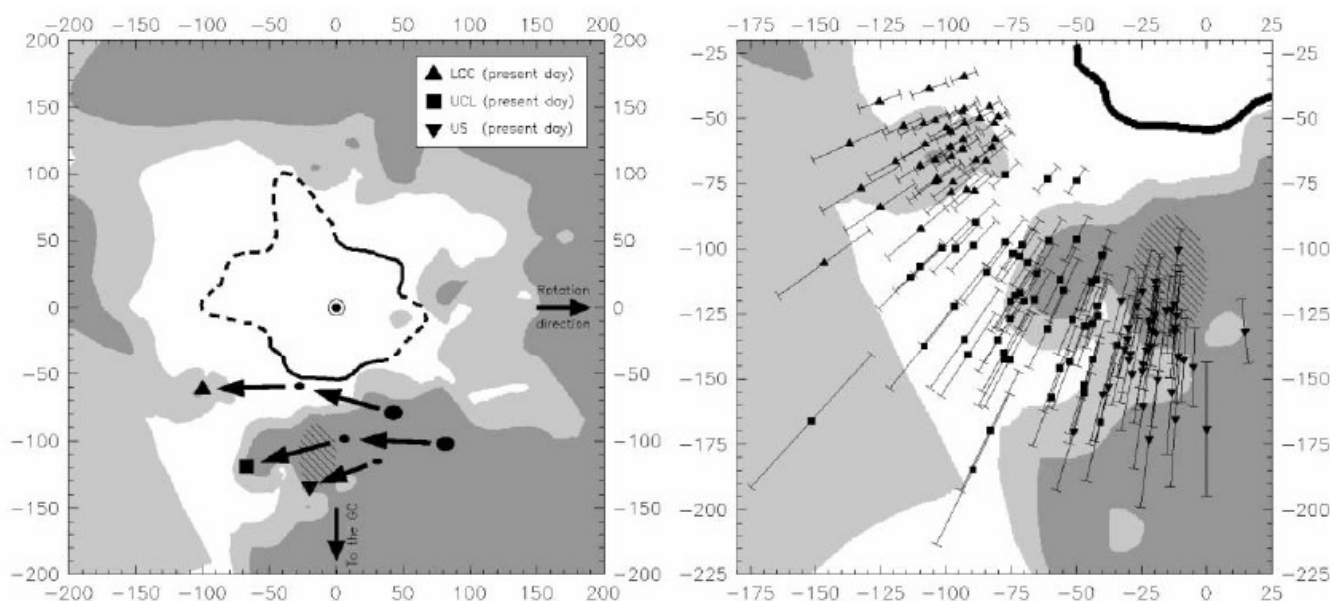


FIG. 1.—*Left*: Local cavity and LB in the plane of the Galactic equator. The filled contours show the Na I distribution (Sfeir et al. 1999), with white used for low-density regions and dark gray for high-density ones. The black contour shows the present size of the LB as determined from X-ray data (Snowden et al. 1998), with the dashed lines indicating contaminated areas where the limits of the LB cannot be accurately determined. The hatched ellipse shows the approximate position of the Ophiuchus molecular cloud (de Geus et al. 1989; Loren 1989a, 1989b). The present and past x - and y -coordinates of the center of the three subgroups of the Sco-Cen association are shown. For LCC and UCL, the past positions shown are those of 5 and 10 Myr ago, while for US only the position of 5 Myr ago is shown. The dimensions of the filled ellipses indicate the uncertainties in the past positions. Coordinates are expressed in units of parsecs. *Right*: Blowup of the left panel with the present positions of the OB stars in each of the three subgroups. Only those stars with accurately determined positions are shown. The symbol used in each case indicates the subgroup membership using the code established in the left panel.

2-3Myrに星の集団が最接近

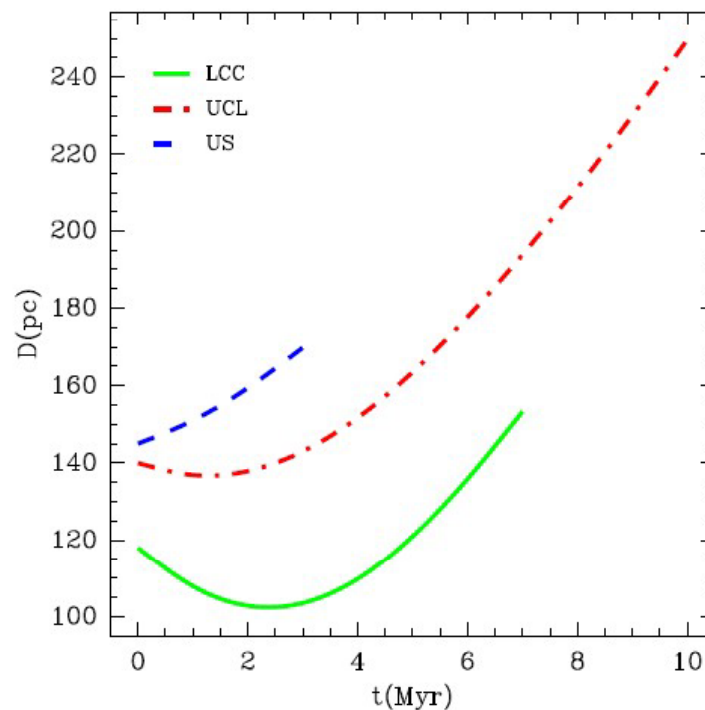


FIG. 1: Evolution of the total distance between the Sun and Sco-Cen subgroups during the last 11 Myr. For each subgroup, only the epoch during which SNe were being formed is shown (see also Fig. 1 of Ref. [2] which shows the projection onto the Galactic Plane of the positions of the Earth and the Sco-Cen association)

2-3Myr前の鉄鉱床に物証を発見？

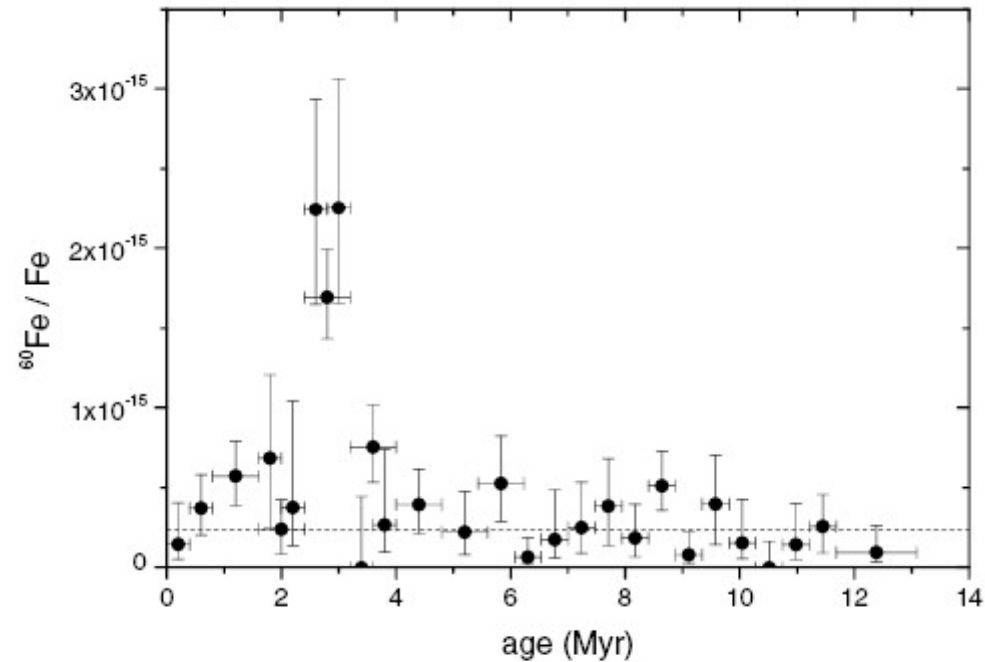


FIG. 1. $^{60}\text{Fe}/\text{Fe}$ ratios versus the age of the layer. The data are not corrected for radioactive decay, background, and uptake of iron into the crust. The vertical error bars correspond to a confidence level of 68.3%; the horizontal error bars indicate the time interval covered by the layer. The background level of 2.4×10^{-16} is indicated by the dashed line.

1. 超新星への衝突

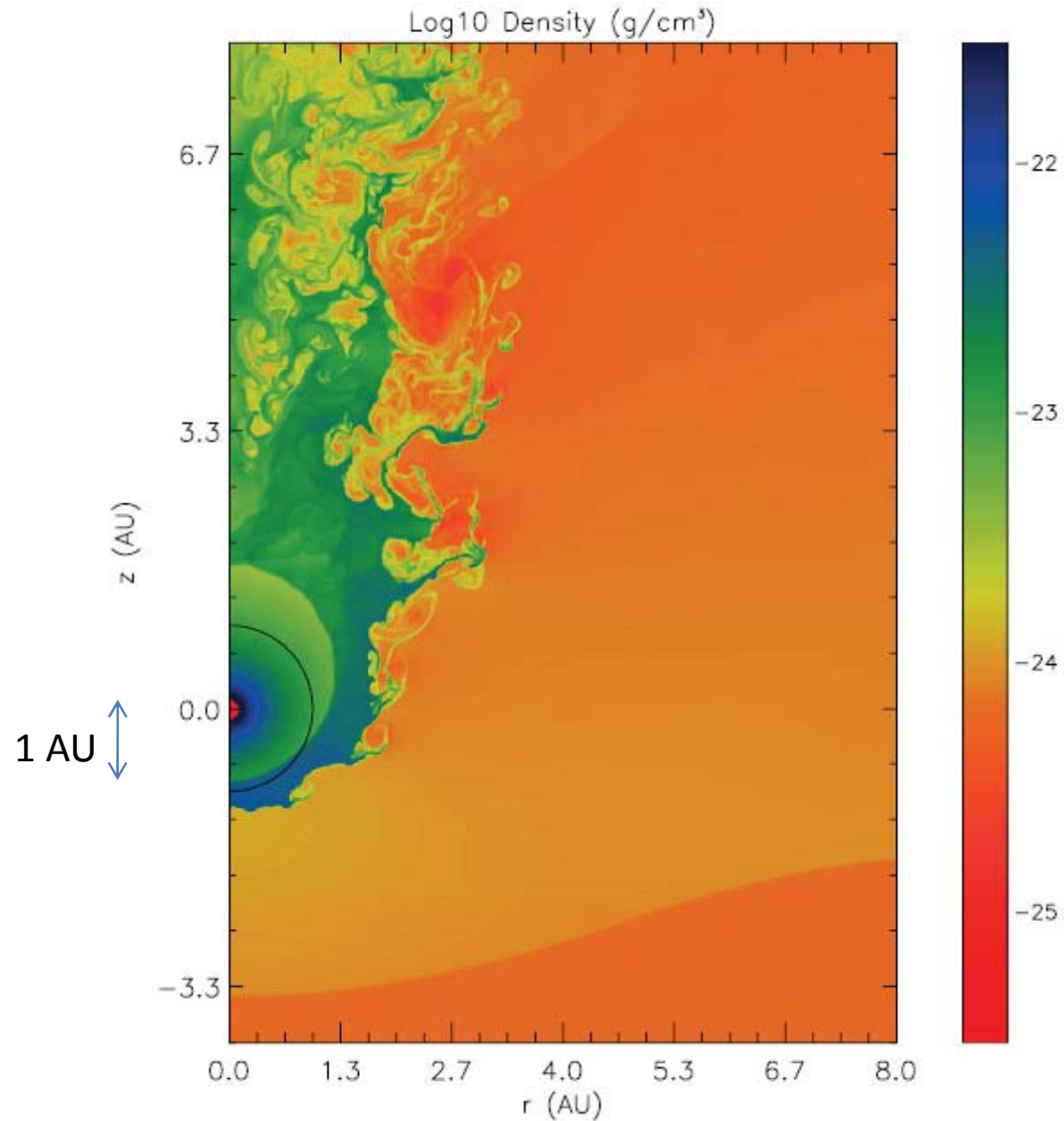
- 猛スピードで広がるため
継続時間は比較的短い
 - 千年スケールで変化
- 太陽圏の極端な圧縮
- 宇宙線の極端な増大
 - 雲による寒冷化
 - 火山噴火
 - 遺伝子ダメージ



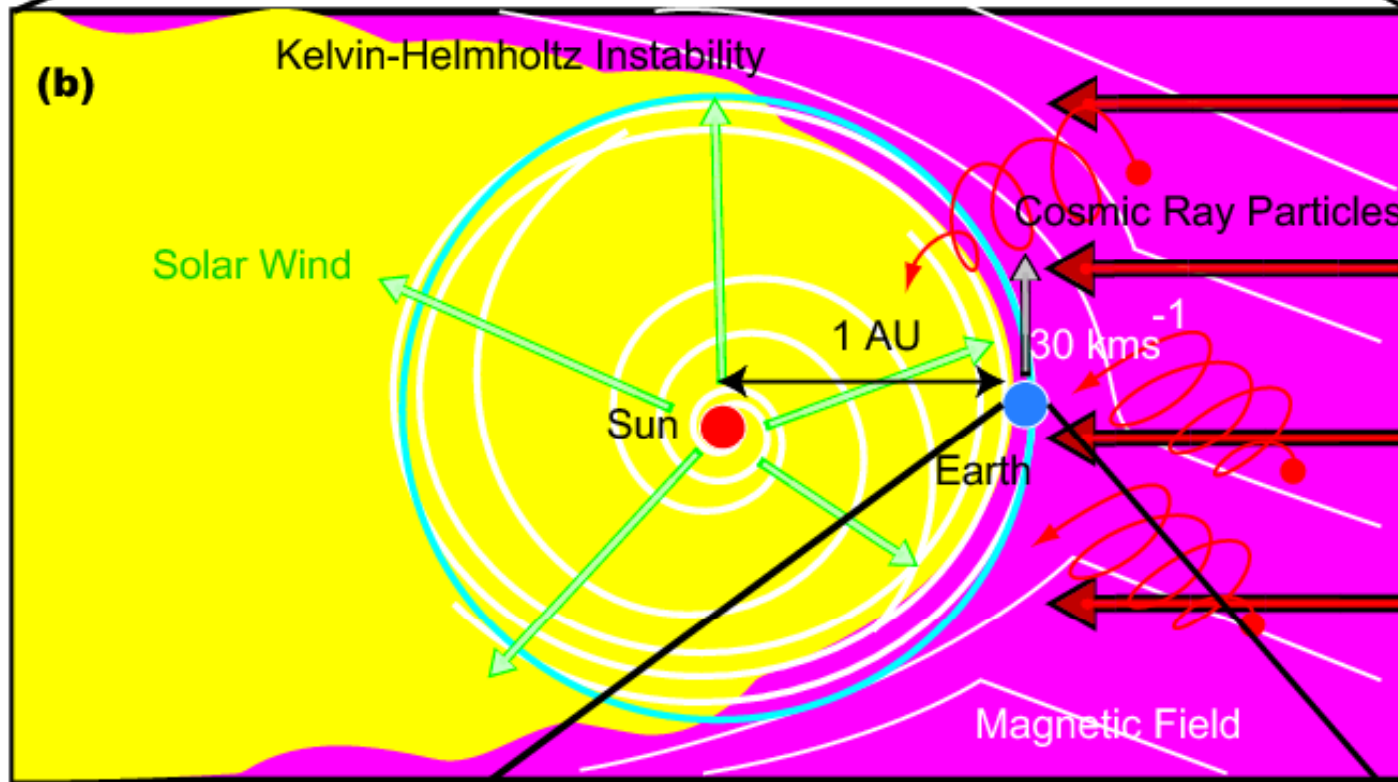
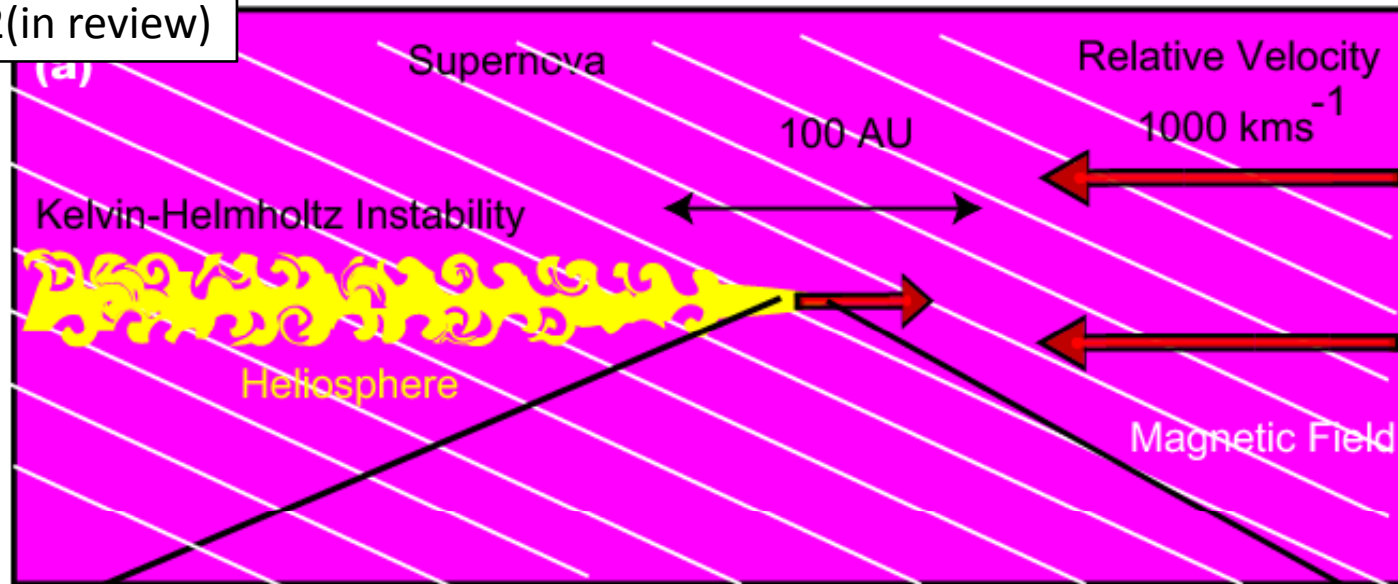
超新星の発生率

- 天の川銀河での発生率
 - 100年で1.5回
 - Cappellaro et al. 1999
- 太陽から10 pc以内で超新星が起きる頻度
 - 10億年で10回
 - Clark et al. 1977
 - 10億年で0.3回
 - Van den Bergh. 1994
 - 10億年で3回
 - Maiz-Apellaniz. 2001

超新星に衝突すると太陽圏が吹っ飛ぶ



(Fields+ 2008 ApJ)



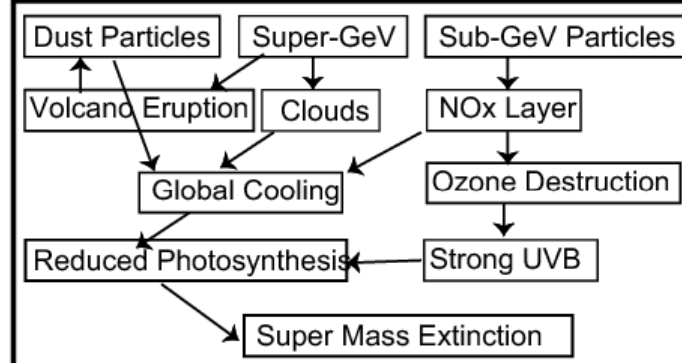
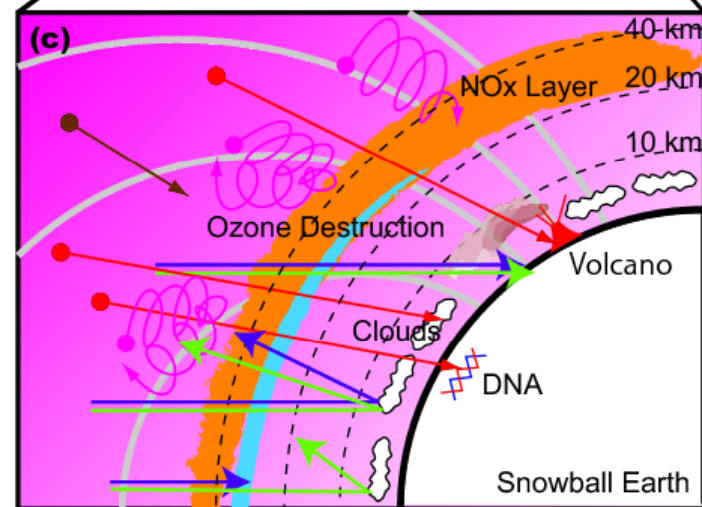
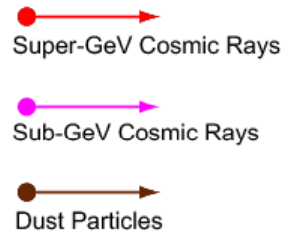
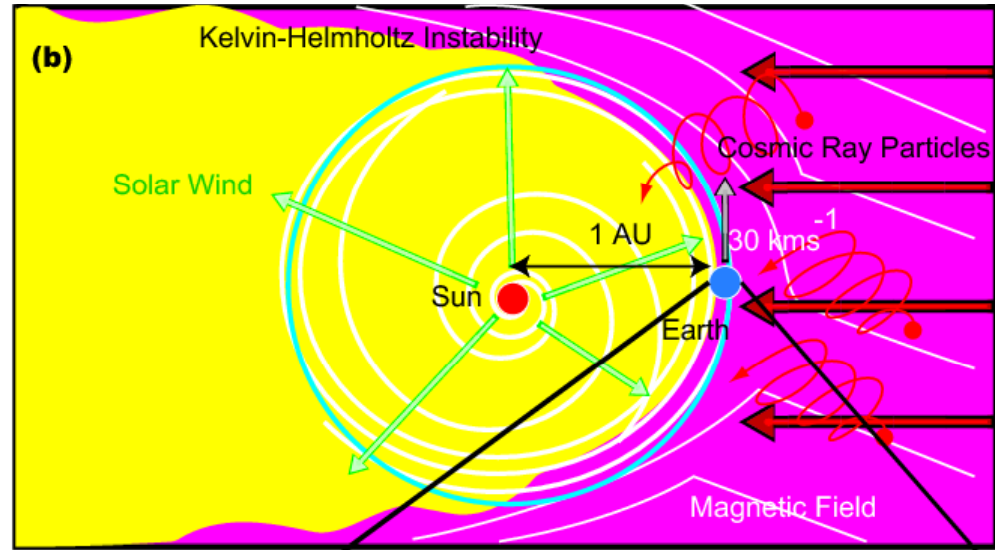
Kataoka+2012(in review)

1. 宇宙線が100-1000倍に

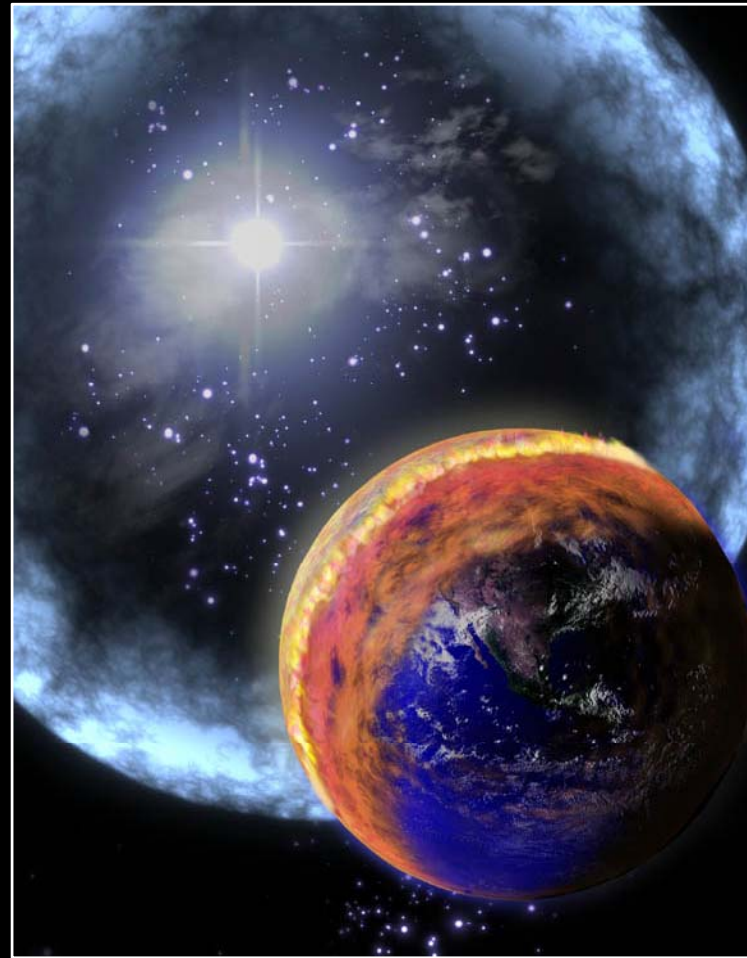
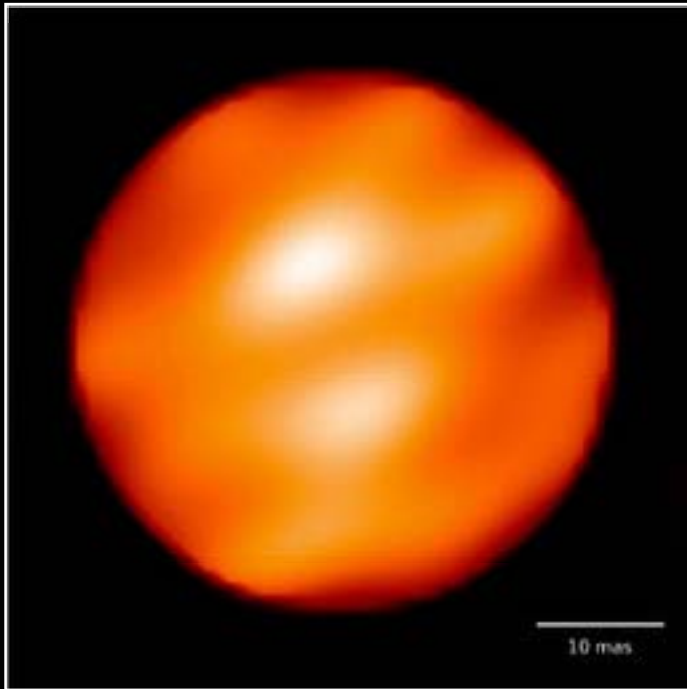
雲だらけになり寒冷化
火山噴火をトリガー

2. オゾン層が全球で破壊

遺伝子ダメージ
光合成が止まる。
海の酸欠状態。
食物連鎖で大絶滅。



ベテルギウスの爆発？



640光年(0.2kpc)と遠いため威力は弱いが一瞬のガンマ線バーストが直撃したら？

ガンマ線バーストによるオゾン破壊の威力

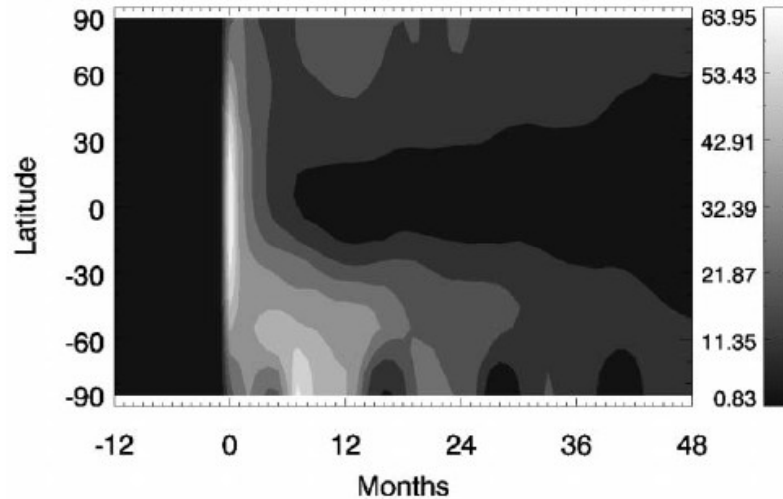


FIG. 1.—Column density of NO_2 in units of 10^{18} cm^{-2} (the burst occurs at month 0). [See the electronic edition of the Journal for a color version of this figure.]

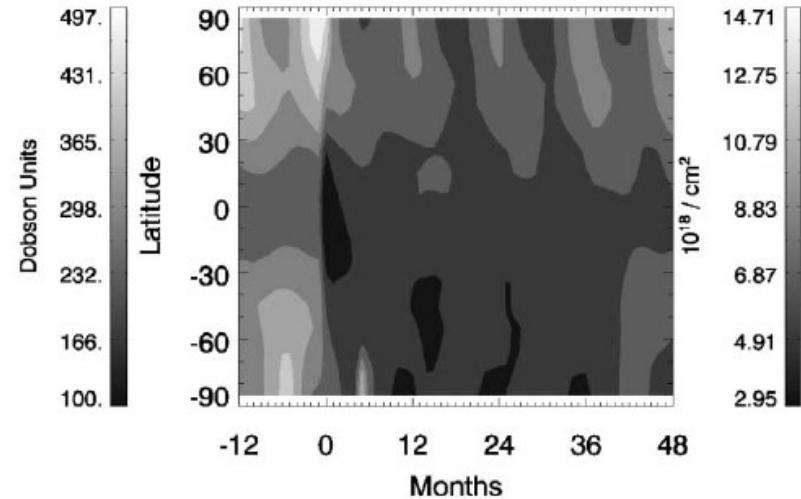


FIG. 2.—Column density of O_3 with scales for both Dobson units (left) and 10^{18} cm^{-2} (right). The burst occurs at month 0. [See the electronic edition of the Journal for a color version of this figure.]

Thomas et al. 2005 ApJ

一瞬のガンマ線バーストによりオゾン層が半減し紫外線は3倍になる。

スーパーフレアもそうだが、100万年スケールの大絶滅には継続時間が短すぎる？

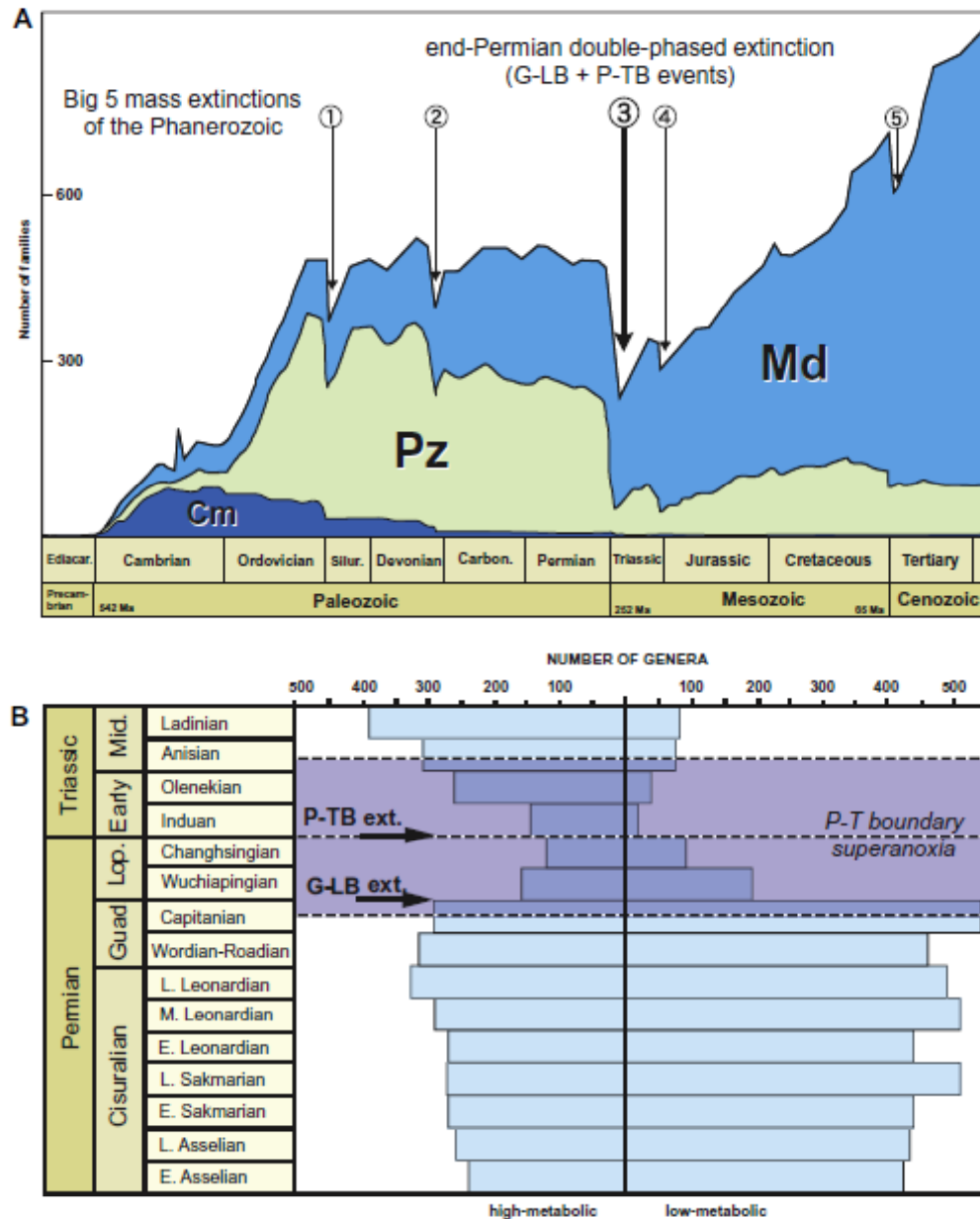


Fig. 1. The Phanerozoic biodiversity change punctuated by major mass extinction events (A, redrawn from Sepkoski, 1984) and the Permo-Triassic details (B, redrawn from Knoll et al., 1996; Isozaki, 1997). The greatest mass extinction in the Phanerozoic comprises two distinct mass extinction events; i.e., one at the Guadalupian-Lopingian boundary (G-LB) and the other at the Permian-Triassic boundary (P-TB). Particularly noteworthy is (1) the sharp decline of marine animals with low metabolic rates (mostly sessile benthos or the Paleozoic fauna by Sepkoski, 1984 as shown in (A) with respect to those with high metabolic rates (animals with gills and strong internal circulation systems; i.e. Modern fauna by Sepkoski) at the G-LB, and (2) the greater magnitude of the selectivity at the G-LB than at the P-TB. Also note the low biodiversity interval from the G-LB to the mid-Anisian (Middle Triassic) for nearly 20 million years by and large overlaps the superanoxic period in the deep-sea (Isozaki, 1997).

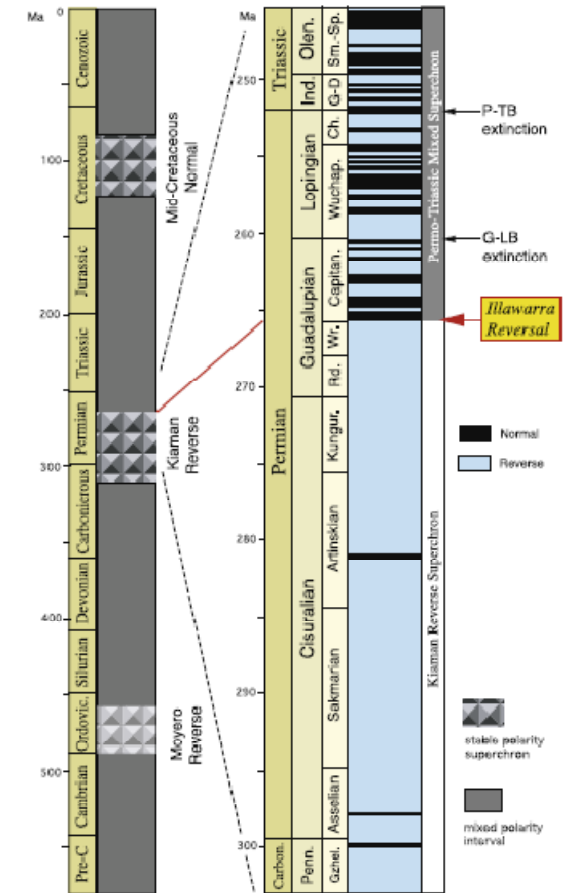


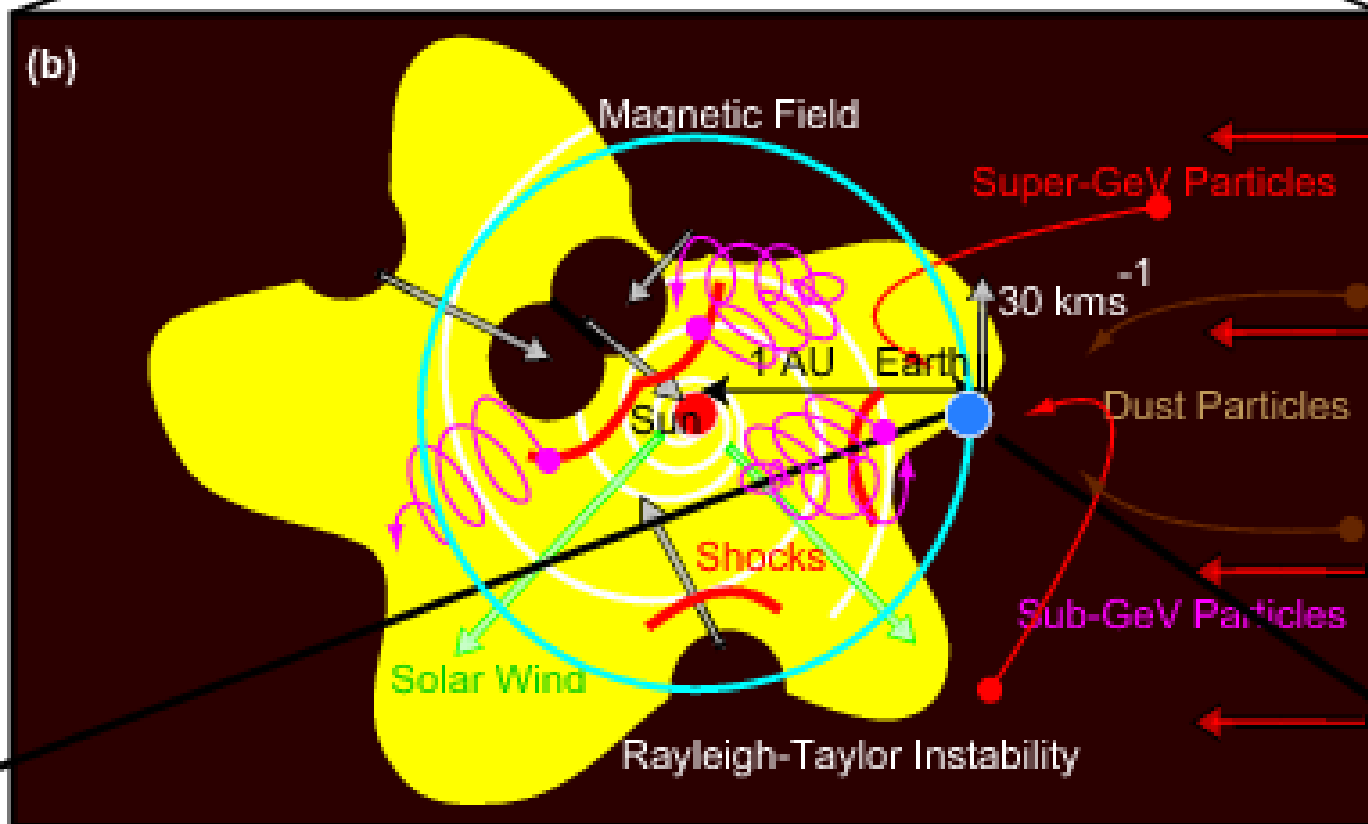
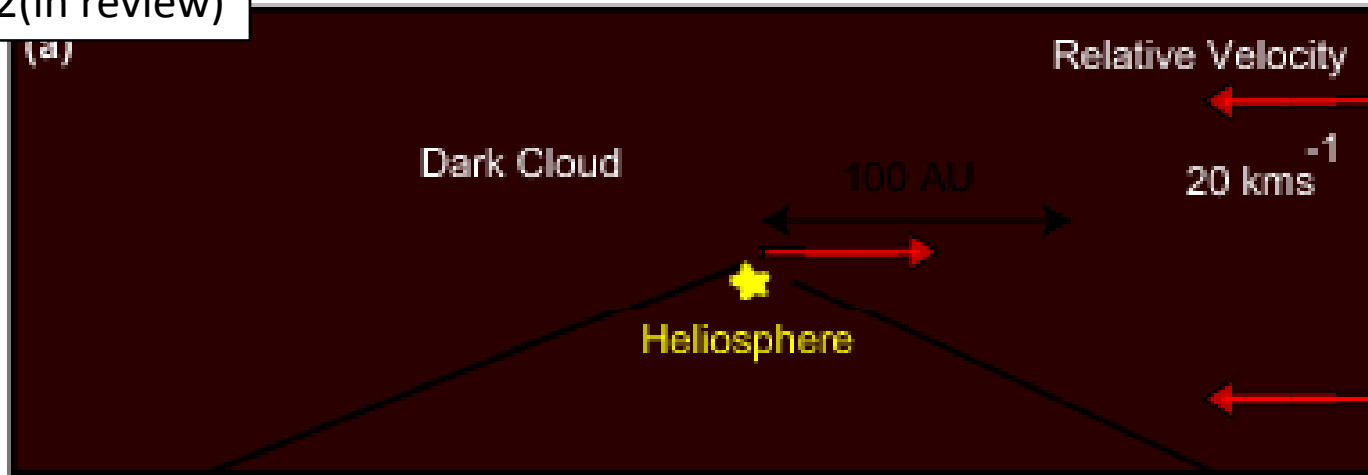
Fig. 2. Geomagnetically unique periods in the Phanerozoic (left) and the Permian magnetostratigraphy punctuated abruptly by the Illawarra Rev (modified from Gradstein et al. (2004) and Courtillot and Olson (2007)). Note the clear contrast between the Kiaman Reverse Superchron (late Cret. Permian) and the Permo-Triassic Mixed Superchron (late Middle Permian to late Triassic). The Illawarra Reversal recorded a sharp change in geomagnetic polarity from a frequently oscillating one. In order to trigger such instability of dipole, a rapid disturbance of thermal conditions is needed. Immediate boundary (D₁ layer). The episodic launching of a mantle superplume coupled with down-welling of a megathrust (subducted slabs) is the most likely disturbance (Fig. 9A). The Mid-Cretaceous Normal Superchron and the Ordovician Moyero Reverse Superchron provide another good examples; among geomagnetic intensity, influx of galactic cosmic radiation, and surface climate of the Earth.

PT境界は実は2回のイベント：
酸欠状態の海、不安定な地磁気、
ケイ酸に富む火山堆積物

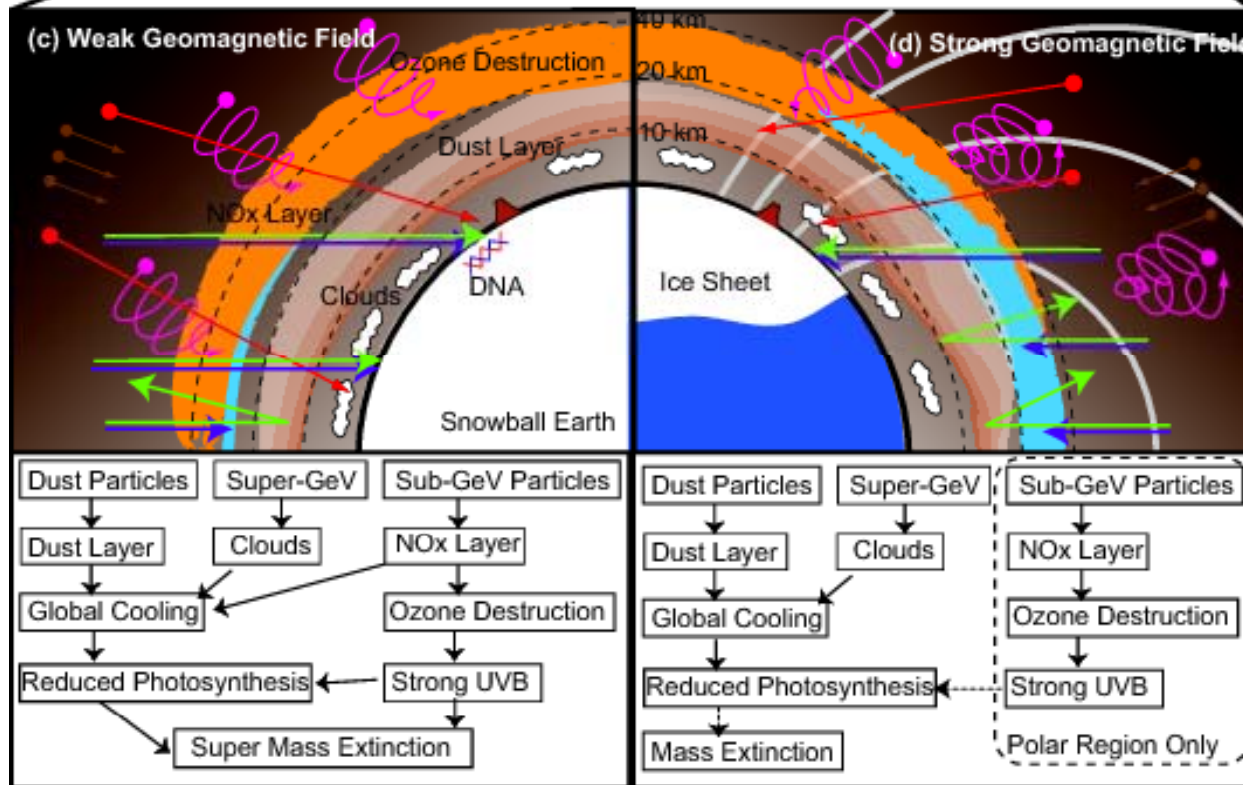
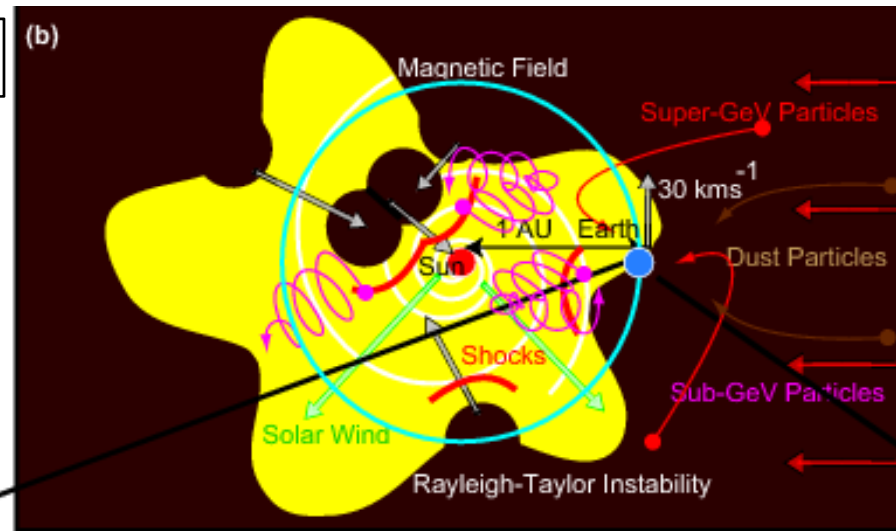
2. 暗黒星雲への衝突

- 一旦入ってしまうと継続時間は百万年スケール
 - 必ず地磁気反転が起きる
- 太陽圏の極端な圧縮
 - 宇宙線によるオゾン破壊
 - NO₂層による寒冷化
- 宇宙塵が成層圏に数年滞在
 - 塵による寒冷化





Kataoka+2012(in review)

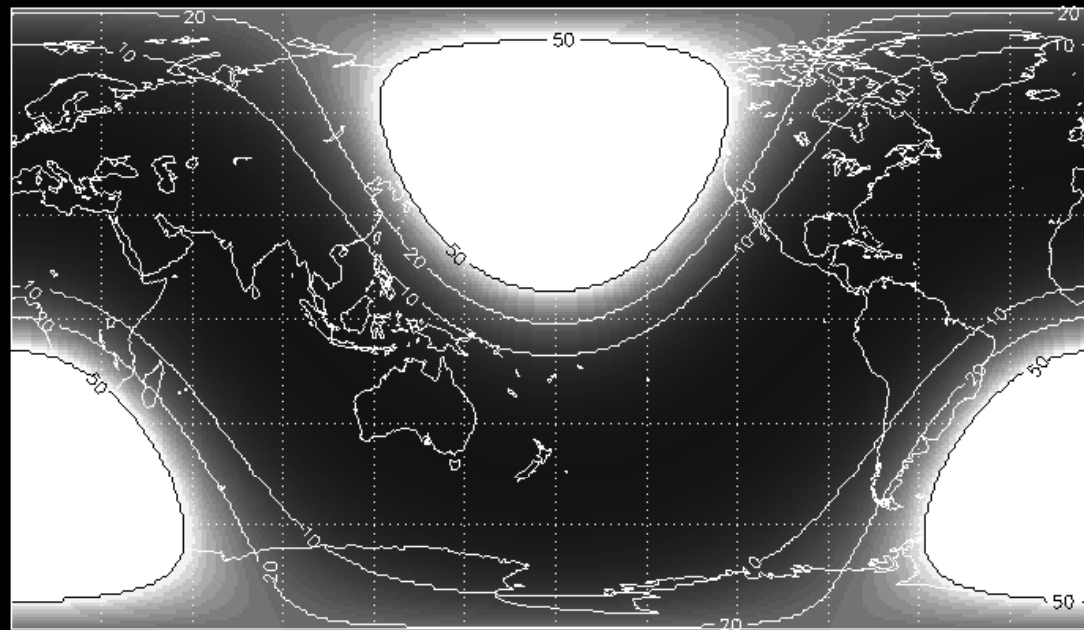


エコシステムの
の全球崩壊

NO₂ 寒冷化は
磁場で防げる

地磁気が1/10になり、45度傾いたときのオゾン破壊

Ozone Reduction(%): 45 deg excursion N_darkcloud = 500/cc



宇宙塵による寒冷化で地球凍結

宇宙塵の量

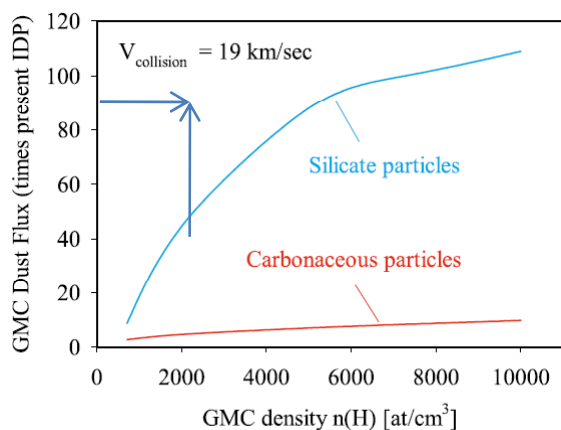


Figure 1. Dust flux into Earth's atmosphere versus hydrogen number density in the GMC. Interstellar particle flux is plotted relative to the present IDP flux [Love and Brownlee, 1993] of 40,000 tons/year. $n(H)$ is the total number density of H and H₂. Velocity of collision was assumed to be 19 km/sec. Silicates have optical properties of "astronomical silicate" [Draine, 1985] and carbonaceous particles have properties of the "amorphous carbon" [Rouleau and Martin, 1991]. Optical properties of the mixed particles (particles grow by coagulation while in the atmosphere) were recalculated following the Maxwell-Garnet rule.

光学的厚さ

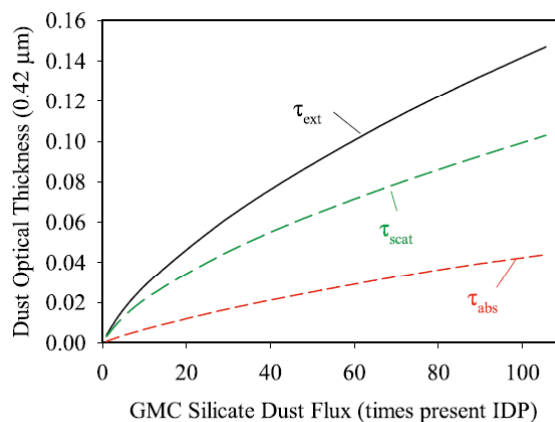


Figure 2. Optical thickness of the interstellar dust layer in Earth's atmosphere versus silicate dust flux. Steady state cumulative optical thickness of the dust layer is plotted at a wavelength of 0.42 μm . Each calculation of τ_{ext} , τ_{scat} and τ_{abs} assumes the flux of carbonaceous dust along with silicates in proportions from Figure 1. Using the maximum value of τ_{abs} (0.04) and the Beer's law it can be demonstrated that the solar forcing at the tropopause level due to absorption on the interstellar dust only should be $\sim -9 \text{ W/m}^2$.

放射強制力

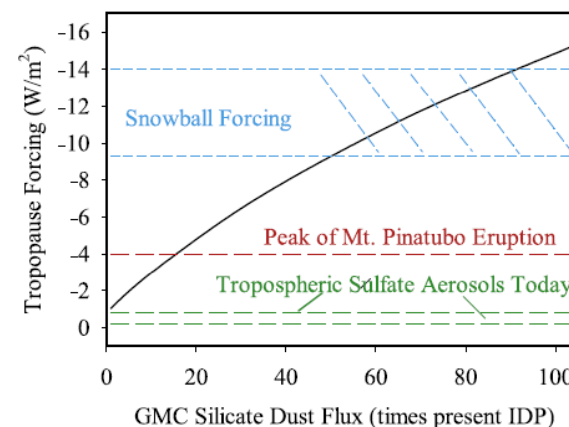


Figure 3. Radiative forcing versus silicate dust flux. Each calculation of the forcing assumes the flux of carbonaceous dust along with silicates in proportions from Figure 1. The net radiative forcing is reported at the tropopause level ($\sim 11 \text{ km}$). Two cyan horizontal lines represent critical solar forcings necessary to trigger runaway ice-albedo feedback that results in global snowball glaciation. Thresholds were determined using the Genesis 2 (3-D global circulation model). The lower threshold was determined assuming that the pre-snowball climate had a mean global surface temperature close to present (287.4 K), the upper threshold assumes that pre-snowball climate was almost completely ice-free (290.4 K). Forcing due to sulfate aerosols from Pinatubo eruption and forcing due to modern tropospheric sulfate aerosols (anthropogenic) are plotted for comparison.



Older Cryogenian ('Sturtian') glacials
730 - 700 Ma



Younger Cryogenian ('Marinoan') glacials
(665 - 635 Ma)

A climate instability caused by ice-albedo feedback

Snowball Earth

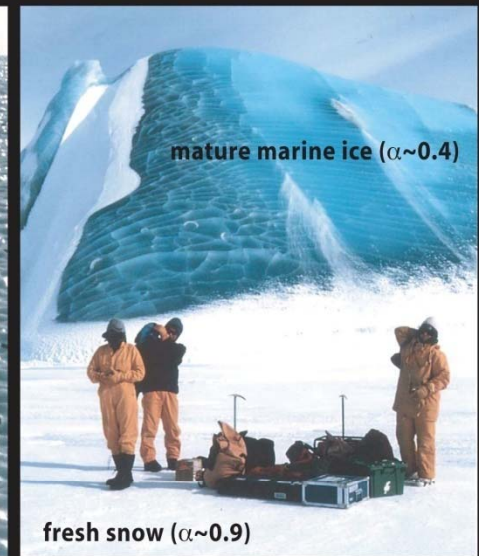
Radiative balance:
 $E_s(1-\alpha) = 4(f \sigma T_s^4)$

<http://www.snowballearth.org/>



Joe Kirschvink

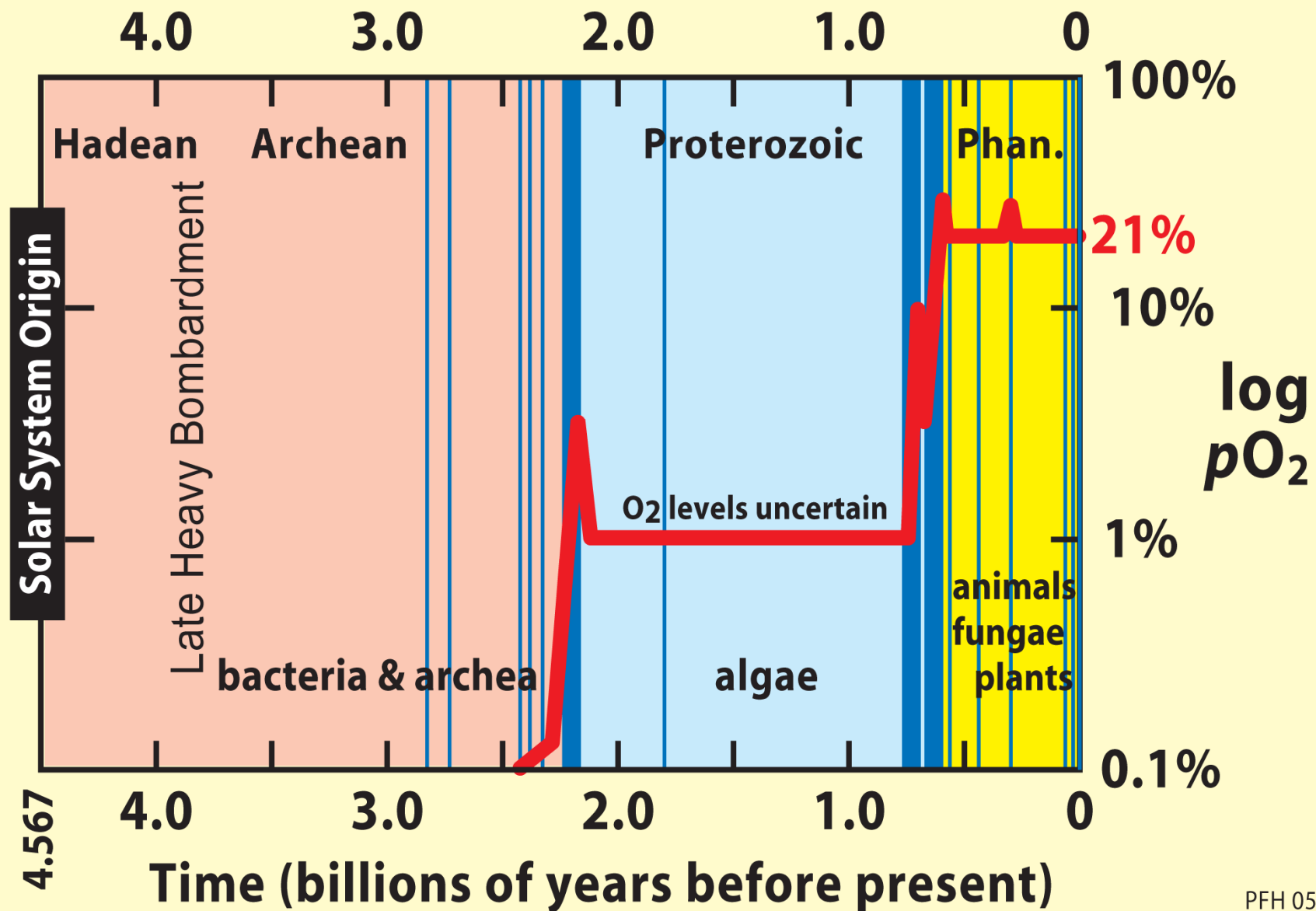
Ice albedo: critical parameter in snowball models

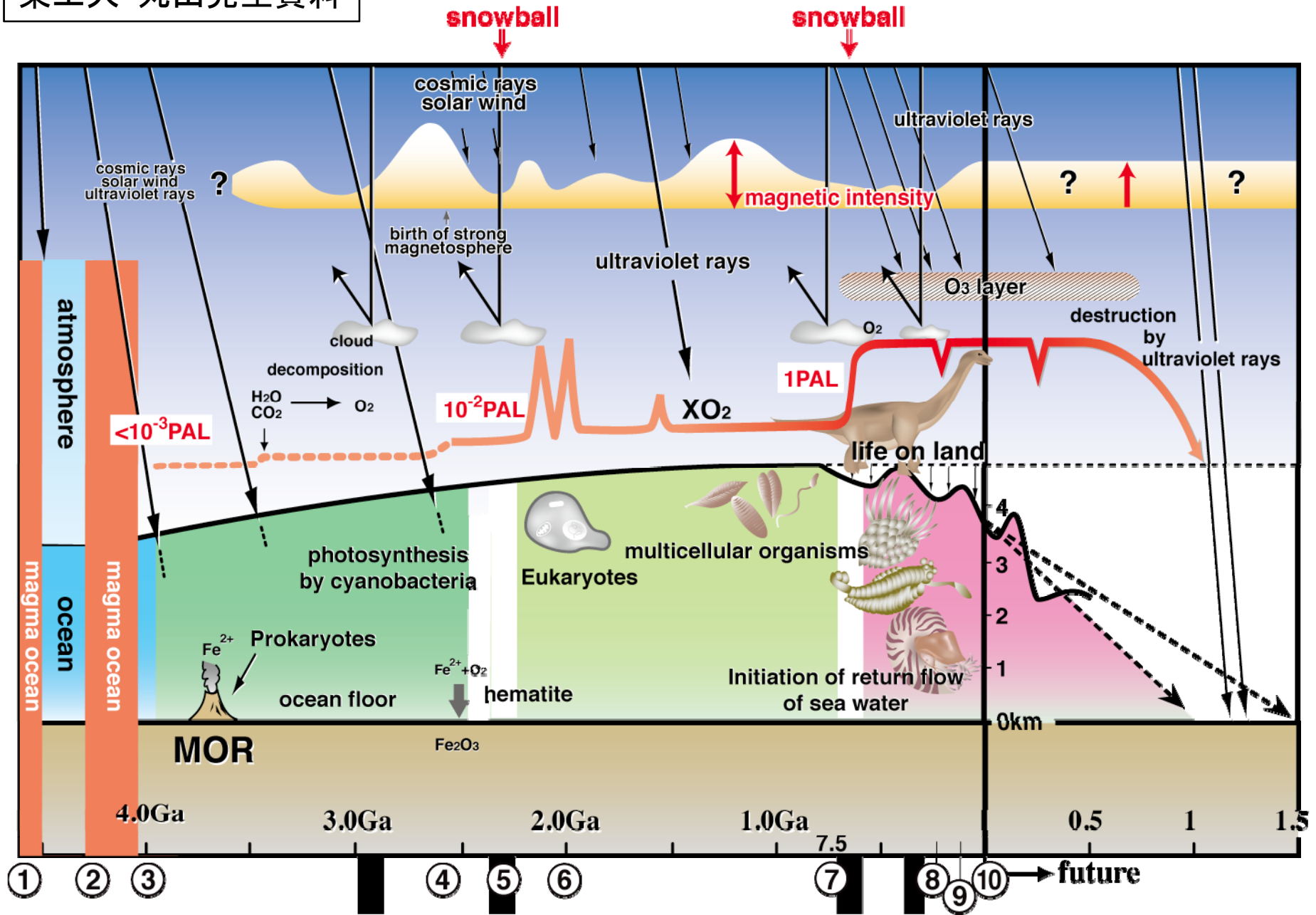


see Warren et al., JGR Oceans 107, 2002.

Steve Warren photos

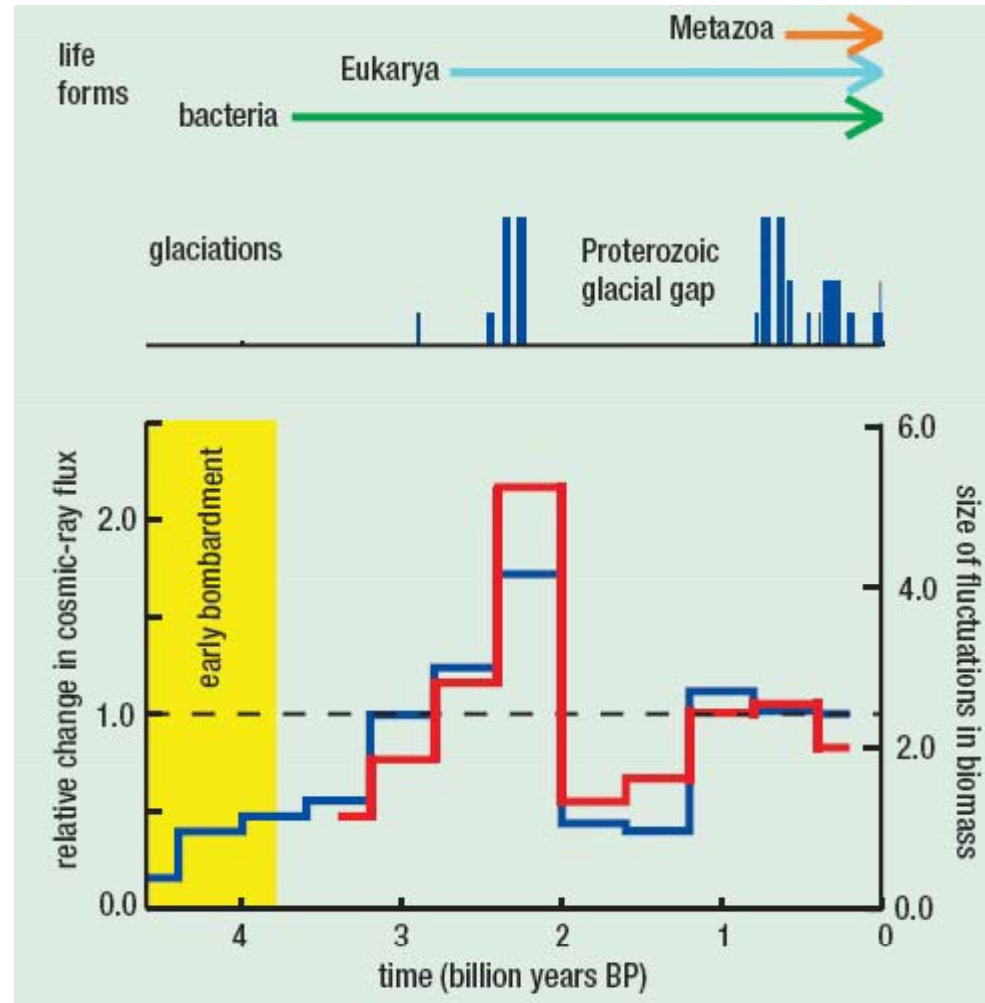
— regional glaciation — global glaciation — oxygen level





スターバースト、雪玉地球、生命誕生

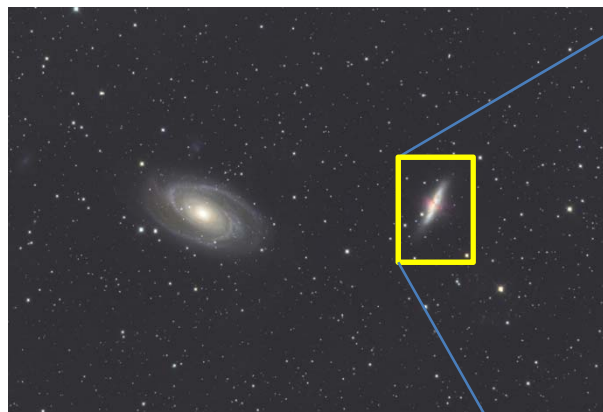
- 地球が凍りつくのは、天の川銀河のスターバーストと同期
 - Shaviv (2003)
 - Svensmark (2007)
 - Rocha-Pinto et al. (2000)
 - Marcos & Marcos (2004)
- ‘Snowball Earth occurred only when star-making peaked. The Galaxy’s baby booms intensified the cosmic rays.’
 - “The Chilling Stars” by Svensmark and Calder



Svensmark (2007)

スターバーストでは、 超新星と暗黒星雲が多発する

	Starburst galaxy	Normal galaxy
Supernova occurrence	Every year	1 per 100 years
Dark cloud in volume	>90%	10%



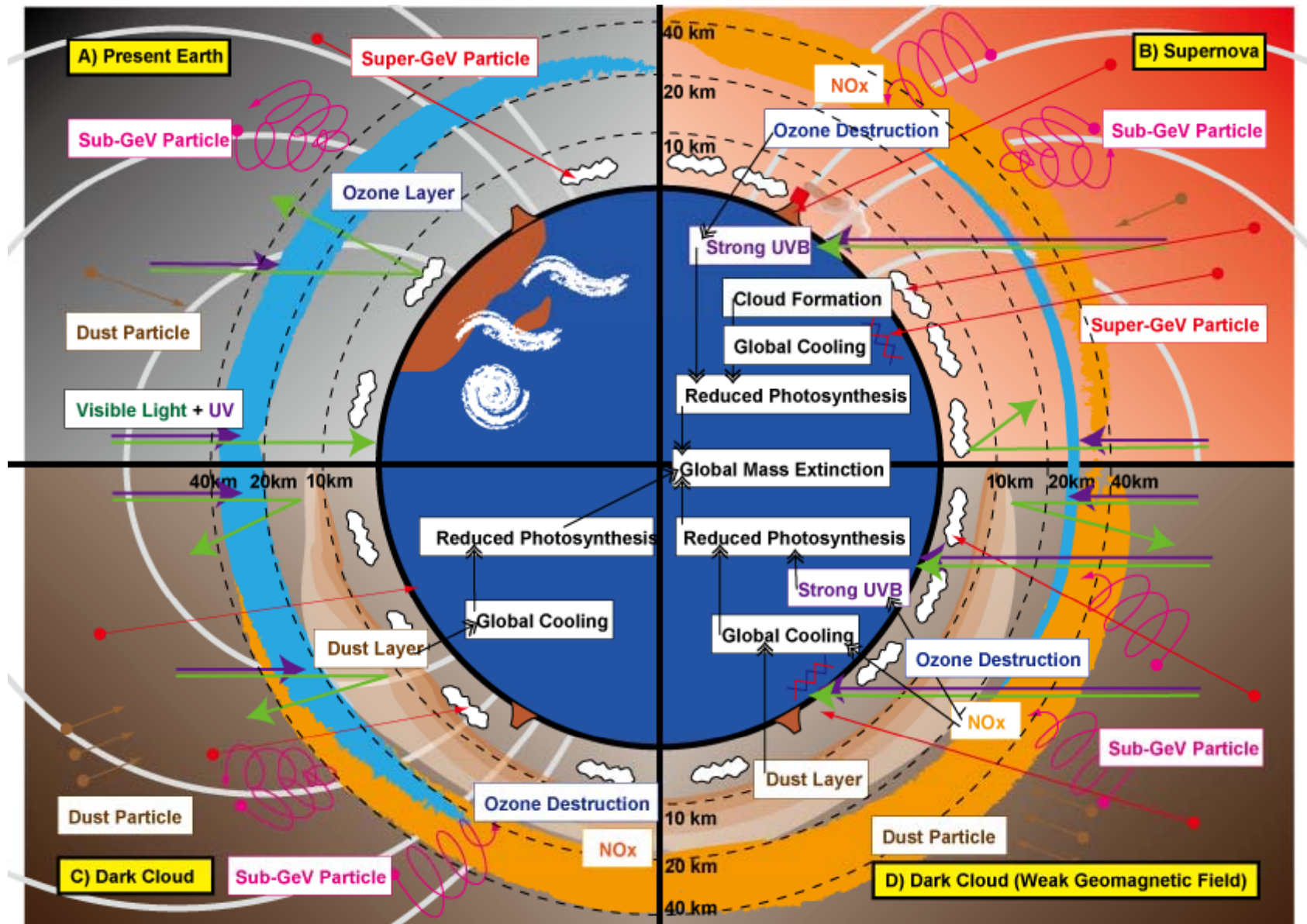
Interaction between galaxies
M81(left) and M82 (right)



Starburst galaxy M82



Normal galaxy NGC4565



過去最悪の宇宙環境まとめ

- 超新星との衝突
 - ガンマ線バーストの放射
- 暗黒星雲との衝突
 - 地磁気反転が同時に発生
- 「3つの槍」と「3つの盾」とのバランスが崩れ、地球が凍りつくような気候変動や、大絶滅、(大進化も！)が起きてきた可能性がある。

第10回アンケート

- 感想は自由に記入してください。
- 最終回で最終レポートを回収します。
 - 提出期限: 7月23日授業中に回収します。
 - 短すぎず長すぎず4ページ程度にまとめること。
 - 図や表を示し、具体的な数字と根拠を出すこと。
 - 必ず文献を引用すること。
 - テーマは自由です。
 - ただし「宇宙と地球の科学」に関係すること。